

Investigating the Jamming Attack on 5G NR Physical Channels

Mohsen Kazemian, *Member, IEEE*

Abstract—This study investigates the jamming attack on the orthogonal frequency-division multiplexing (OFDM) based physical channels in 5G new radio (NR) technology from the aspect of signal processing. Disrupting the orthogonality property between subcarriers (SCs) is considered as one of the jammers' targets in OFDM based generations. Focusing on the orthogonality property, we propose a method to detect the attacked subcarriers, and then neutralize the jamming attack using a multiplicative signal. Thanks to studying the frequency aspect of the attacked signal, the proposed method is independent of the jammers' transmitted power. Simulation results evaluate the detection performance of the proposed method with various numbers of OFDM subcarriers.

Index Terms—Jamming, Physical layer, 5G NR, OFDM, Security.

I. INTRODUCTION

Fifth generation new radio (5G NR) is developed by the 3rd generation partnership project (3GPP) as a radio access technology (RAT) for the 5G cellular networks. 5G NR operates on the higher bands between either 410 MHz–7125 MHz or 24250 MHz–52600 MHz. Lower latency, greater user capacity, network slicing, and enhanced speed are the superiority of this technology over the previous generations [1], [2], [3], [4].

Dynamic structure and removal of sparse control channels such as physical control format indicator channel (PCFICH) are two main reasons that make 5G NR as a far less vulnerable technology compared to long term evolution (LTE) standard. Jamming attacks can only be neutralized at the physical layer, but not at the medium access control (MAC) or network layer [5].

In 5G NR, uplink and downlink resources are assigned at an orthogonal frequency division multiplexing (OFDM) symbol level [6], [7], [8]. Jammers cause an undesired denial of service (DoS) and interrupt the communications between the legitimate users and the corresponded base stations (BSs). Several scenarios can be used in this regard. The main principle to attack a channel is disrupting the orthogonality property between the OFDM spectrums by adding a phase or frequency offset to the legitimate signal. In this case, the subcarriers (SCs) experience the overlapping phenomenon and the transmitted signal will be lost entirely. The other possibilities are: 1) transmitting radio signals with the aim of decreasing signal-to-noise ratio (SNR) at the legitimate user side, 2) continually occupying the transmission channel to famish transmissions initiated by legitimate users, and, 3) disabling channel estimation by forcing the received energy at

the pilot OFDM samples to zero, using a fake signal similar to the legitimate one.

Physical broadcast channel (PBCH) and physical downlink control channel (PDCCH) are respectively the most vulnerable channels in 5G NR in terms of both attack efficiency and complexity [9].

PBCH conveys critical information of the cell, called master information block (MIB), which includes essential information to initiate a connection between the user equipment (UE) and the corresponded cell. PBCH occupies the second and the fourth OFDM symbols (i.e., four symbols in each slot), covering 240 subcarriers (i.e., 20 resource blocks (RBs)) in each symbol time. Furthermore, PBCH is assigned to 48 subcarriers, allocated to the below and the above of secondary synchronization signal (SSS) in the third OFDM symbol. Thus, PBCH occupies 576 resource elements (REs) per synchronization signal block (SSB), including REs for PBCH payload (i.e., 432 REs) as well as REs for demodulation reference signals (DMRS) (i.e., 144 REs). PBCH DMRS is required for coherent demodulation of PBCH payload. The SSB structure consisting of PBCH, primary synchronization signal (PSS) and SSS is described in Fig. 1.

Since unlike LTE, cell specific reference signal (CRS) is not defined in 5G NR, PBCH DMRS is a vital signal for PBCH decoding. PBCH DMRS is considered as the most efficient target from the jammers' point of view, due to the following reasons: 1) it is generated by pseudo-random sequence and determined by SSB, which broadcasts periodically and is unencrypted during the initial access, 2) as it only occupies 25% of the PBCH resources, a malicious transmitter requires a lower level of jamming power to target it than to attack the entire PBCH block, and, 3) PBCH DMRS is in the same spot every frame.

After PBCH DMRS and PBCH, PDCCH ranks third in terms of vulnerability. This physical channel transmits downlink control information (DCI) as the core of the physical control channel of the 5G network to control the transmission and reception of uplink and downlink data [10]. Physical random access channel (PRACH) and physical uplink control channel (PUCCH) are respectively placed in the next ranks. The former is used by UE to request a connection setup known as random access. PUCCH is assigned for uplink control information, including: 1) hybrid automatic repeat request (HARQ) feedback acknowledgments to indicate the success of the downlink transmission, 2) scheduling request to seek the time-frequency resources from cellular network for uplink transmission, and, 3) downlink channel-state information (CSI) for link adaptation.

The importance of physical layer security motivates re-

M. Kazemian is with the Department of Electrical Engineering, Yazd University, Yazd, Iran, (e-mail:mohsenkazemian@yazd.ac.ir).

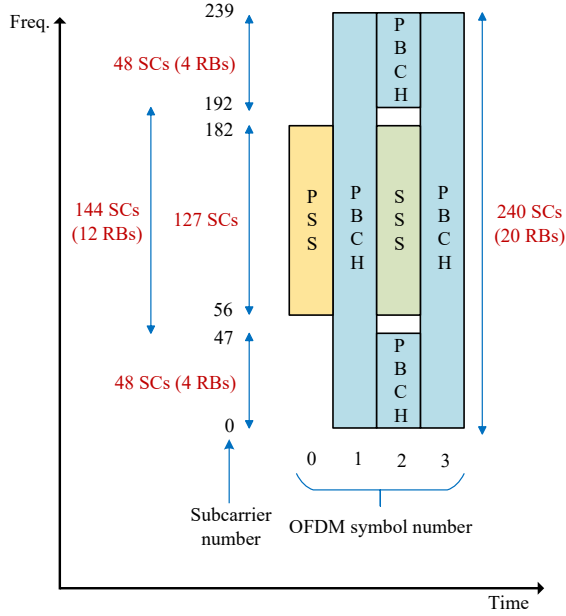


Fig. 1. The time-frequency structure of SSB.

searchers to move in this direction. The method in [11] develops a feature-based classification model using conventional machine learning (ML) algorithms. Similar works that use ML methods are not successful in case of insufficient training samples [12], [13]. [14] works on the passive jamming on downlink cell-free massive multiple-input multiple-output (MIMO) systems. This work broadcasts artificial noise to disrupt the jamming signal. It proposes a cooperative physical layer security algorithm to facilitate artificial noise broadcasting via access point cooperation. Then, it presents an independent physical layer security algorithm to almost retake the consumed power using access points with independent artificial noise broadcasting. Obviously, the power consumption problem is the drawback of this method. The method in [15] is designed for only the particular adaptive modulation OFDM systems, and, finally, [16] studies the maximization problem of signal-to-interference plus noise ratio (SINR), which is infirm against low power jamming attacks.

OFDM is used on both uplink and downlink of 5G NR standard and it seems to be an inseparable scheme for the third generation of mobile networks onwards. In this study, we investigate the loss of orthogonality (LoO) property in the 5G NR physical channels, and then propose a method for jamming cancellation at the user side. The contributions of this study are as follows: 1) thanks to deploying the method at the user side, this work is independent of the number of jammers, 2) no additional hardware is required, and, 3) due to our focus on the frequency aspect, the power of jamming signal does not affect the performance of our method. The considered system model is shown in Fig. 2.

II. JAMMING PRINCIPLE

In OFDM systems, LoO between subcarriers leads to inter-carrier interference (ICI), and further results in severe DoS for the users. In the following, we study an attacking scenario

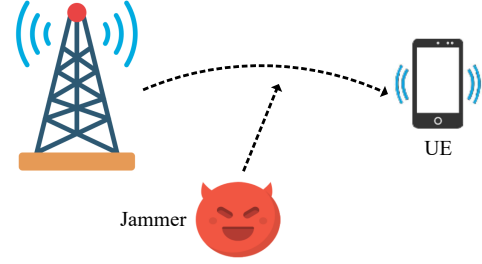


Fig. 2. The considered system model.

where a jammer shifts the frequencies of the subcarriers, causing misalignment of the spectral nulls. This phenomenon results in ICI.

N -point inverse fast Fourier transform (IFFT) at the transmitter side generates one OFDM symbol as follows:

$$x_n \triangleq \frac{1}{N} \sum_{k=0}^{N-1} X_k e^{jn w_k}, \quad n = 0, \dots, N-1, \quad (1)$$

where k , n and $w_k \triangleq \frac{2\pi k}{N}$ are the frequency index, time index, and the k th radian frequency component, respectively. $X_k \triangleq A_k e^{j\psi_k} \in \mathbb{C}$ is the transmitted symbol on the k th subcarrier (i.e., k th frequency component) with amplitude A_k and phase ψ_k . Thus, x_n consists of N subcarriers (i.e., N values for A_k , ψ_k and w_k).

Let $O_{ki} \triangleq \frac{1}{N} \sum_{n=0}^{N-1} c_k c_i^*$. The orthogonality condition for two different subcarriers $c_k \triangleq X_k e^{jn w_k}$ and $c_i \triangleq X_i e^{jn w_i}$, $k \neq i$, is defined by the following equation:

$$\begin{cases} \text{Orthogonal} & \text{if } O_{ki} = 0, \\ \text{Non-orthogonal} & \text{otherwise.} \end{cases} \quad (2)$$

Since SSB is unencrypted during the initial access, the jammer can simply acquire the value of N . If \tilde{c}_i denotes the attacked c_i by a malicious jammer with the signal $a_m = X_m e^{jn w_m}$, then $\tilde{O}_{ki} \triangleq \frac{1}{N} \sum_{n=0}^{N-1} c_k \tilde{c}_i^*$ yields:

$$\begin{aligned} \frac{1}{N} \sum_{n=0}^{N-1} X_k e^{jn w_k} \sum_{m=0}^{N-1} X_m^* e^{jn w_{-i}} \\ = \frac{1}{N} X_k X_i^* X_m^* \mathcal{H}_{k,i}, \end{aligned} \quad (3)$$

where $\mathcal{H}_{k,i} \triangleq \sum_{n=0}^{N-1} e^{jn w_{k-i}}$ and $\tilde{i} \triangleq i + m$. Using the following equation:

$$\sum_{i=0}^{N-1} e^{-j d w_i} = \begin{cases} N & \text{for } d = z \times N, z \in \mathbb{Z}, \\ 0 & \text{otherwise,} \end{cases} \quad (4)$$

we have:

$$\tilde{O}_{ki} = \begin{cases} A_k \times A_i^* \times A_m^* & \text{for } \frac{k-\tilde{i}}{N} = z \in \mathbb{Z}, \\ 0 & \text{otherwise.} \end{cases} \quad (5)$$

Algorithm 1 The proposed anti-jamming scheme for OFDM-based physical channels.

Input: $c_k \triangleq X_k e^{jnw_k}$, $c_i \triangleq X_i e^{jnw_i}$, $a_m \triangleq X_m e^{jnw_m}$ and N ,

- 1: **for** $i = 0$ to $N - 1$,
- 2: Compute $\psi(i) \triangleq \sum_{k=1}^{N-1} \mathbf{1}\{\mathbf{Tr}(\mathbf{A}_{k,i}) \neq 0\}$,
- 3: **if** $\psi(i) = N - 1$, **then**
- 4: **Return:** i th subcarrier is under attack,
- 5: **end if**
- 6: **end for**
- 7: **if** $m' + k + \tilde{i} \neq zN$, **for** all $k \in \{0, \dots, N - 1\}$, **then**
- 8: **Return:** m' ,
- 9: **else** Update m' ,
- 10: **end if**

Output: $c_{m'} \triangleq X_{m'} e^{jnw_{m'}}$.

III. ANTI-JAMMING STRATEGY

In this section, we detect the attacked subcarriers, the ones that have lost the orthogonality property, and then we propose multiplication of a new signal by the received signal at the user side, with the aim of jamming cancellation. Let $\mathbf{e}^m \triangleq \{e^0, e^{jw-m}, \dots, e^{j(N-1)w-m}\}^T$, $\mathbf{e}^{k,i} \triangleq \{e^0, e^{jw_{k-i}}, \dots, e^{j(N-1)w_{k-i}}\}$, and $\mathbf{A}_{k,i}^{N \times N} \triangleq \mathbf{e}^m \times \mathbf{e}^{k,i}$. Referring to (3) and (5), $\mathcal{H}_{k,i} = \mathbf{Tr}(\mathbf{A}_{k,i})$, and, if the i th subcarrier is attacked by a jammer, then $\mathbf{Tr}(\mathbf{A}_{k,i}) \neq 0$. Therefore, in order to determine the i th subcarrier that is under a jamming attack, we propose the following test:

$$\psi(i) \triangleq \sum_{k=1}^{N-1} \mathbf{1}\{\mathbf{Tr}(\mathbf{A}_{k,i}) \neq 0\}, \quad (6)$$

where $\mathbf{1}\{\cdot\}$ is the indicator function, and $i, k \in \{0, \dots, N - 1\}$. Equation (6) consists of $\tilde{N} \triangleq \frac{N!}{2!(N-2)!}$ non-repetitive executions to test each subcarrier with the other $N - 1$ subcarriers. Therefore, we determine the i th disrupted subcarrier using the following statement:

$$\begin{cases} \text{LoO} : & \psi(i) = N - 1, \\ \text{No fully LoO} : & \text{otherwise,} \end{cases} \quad (7)$$

where no fully LoO refers to the situation in which alignment of all the spectral nulls is not entirely missed.

Remark 1: Equation (5) declares that the condition for the occurrence of LoO between c_i and c_k is $\frac{k-i}{N} = z \in \mathbb{Z}$. However, this condition (i.e., results in LoO) may be caused by one or both of the following reasons: 1) a jamming attack has occurred, 2) the value of N is not chosen correctly and needs to be updated.

The anti-jamming approach is based on multiplication of signal $c_{m'} \triangleq X_{m'} e^{jnw_{m'}}$ by the i th subcarrier such that $m' \neq zN - (k + i)$, for any $k \in \{0, \dots, N - 1\}$ and $z \in \mathbb{Z}$. We summarize the design steps of our proposed method to detect and neutralize a jamming attack as the pseudo-code in Algorithm 1.

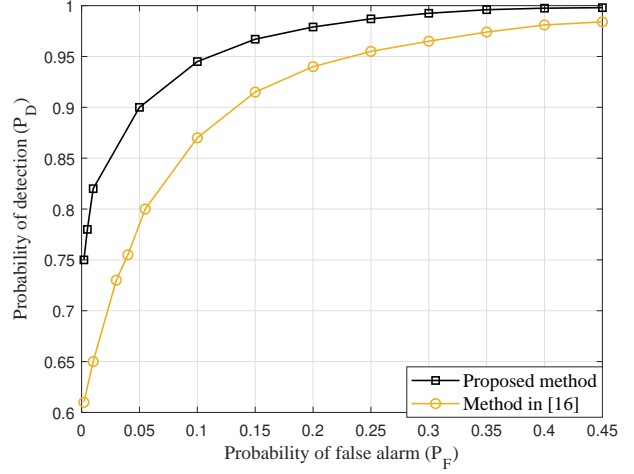


Fig. 3. The detection performance of the proposed method compared with [16] for various N values.

IV. SIMULATION RESULTS

In this section, we illustrate the simulation results of the proposed detection method using receiver operating characteristic (ROC) curve. ROC is the plot of the detection probability (P_D) versus the false alarm probability (P_F) at each threshold setting. We consider clustered delay line (CDL)-D model with the parameters according to 3GPP 38.901 [17], and subcarrier spacing of 15kHz. The UE and the jammer are uniformly distributed into $(-2\pi, 2\pi)$ and the BS is located at the center of this circular region. Furthermore, jamming to signal ratio (JSR) and SNR are set to 0dB and 5dB, respectively.

Referring to Remark 1, LoO is not only the result of a jamming attack. Fig. 3 depicts the superiority of the proposed method over the competing method in [16], in the aspect of detection performance. This figure is achieved using $N = 256, \dots, 2048$ to consider the effect of different subcarrier numbers. The future efforts in this direction will be conducted in a real-time system, to estimate all the attacked subcarriers, while only a few of them are available.

V. CONCLUSION

In this study, we have investigated the LoO phenomenon in the 5G NR physical channels, which is occurred by a malicious attacker. Firstly, we used the non-orthogonality condition to detect the attacked subcarriers at the user side, and then a multiplicative signal was proposed to neutralize the jamming attack. Simulation results evaluate our proposed method with the different number of subcarriers and prove its detection superiority over a recent method. Vulnerability of OFDM-based physical channels, specially PBCH and PDCCH, motivates researchers to further studies in this direction.

REFERENCES

- [1] R. K. Saha and J. M. Cioffi, "Dynamic spectrum sharing for 5G NR and 4G LTE coexistence - A comprehensive review," *IEEE Open Journal of the Communications Society*, vol. 5, pp. 795–835, Jan. 2024.

- [2] D. López-Pérez, A. De Domenico, N. Piovesan, G. Xinli, H. Bao, S. Qitao, and M. Debbah, "A survey on 5G radio access network energy efficiency: Massive MIMO, lean carrier design, sleep modes, and machine learning," *IEEE Communications Surveys and Tutorials*, vol. 24, no. 1, pp. 653–697, Jan. 2022.
- [3] S. Sabapathy, J. S. Prabhu, S. Maruthu, and D. N. K. Jayakody, "Profuse channel estimation and signal detection techniques for orthogonal time frequency space in 6G epoch: A survey," *IEEE Access*, vol. 11, pp. 129 963–129 993, Nov. 2023.
- [4] R. K. Saha and J. M. Cioffi, "Correction to "dynamic spectrum sharing for 5G NR and 4G LTE coexistence—a comprehensive review"," *IEEE Open Journal of the Communications Society*, vol. 5, pp. 1275–1275, Feb. 2024.
- [5] H. Tan, Z. Li, N. Xie, J. Lu, and D. Niyato, "Detection of jamming attacks for the physical-layer authentication," *IEEE Transactions on Wireless Communications*, vol. 22, no. 12, pp. 9579–9594, Dec. 2023.
- [6] M. Kazemian, P. Varahram, S. Jahari Bin Hashim, B. B. M. Ali, and R. Farrell, "A low complexity peak-to-average power ratio reduction scheme using Gray codes," *Wireless Personal Communications*, vol. 88, pp. 223–239, May 2016.
- [7] M. Kazemian, P. Varahram, B. B. M. Ali, and S. Mohammady, "A low complexity PAPR reduction scheme based on radix-II IFFT," in *2015 IEEE International Conference on Consumer Electronics (ICCE)*, 2015, pp. 420–421.
- [8] M. Yıldırım, "Subcarrier-interactive dual-mode OFDM," *IEEE Communications Letters*, vol. 27, no. 5, pp. 1472–1476, Feb. 2023.
- [9] A. Chakrapani, "On the design details of SS/PBCH, signal generation and prach in 5G-NR," *IEEE Access*, vol. 8, pp. 136 617–136 637, Jul. 2020.
- [10] S. Varatharajan, M. Grossmann, and G. Del Galdo, "5G new radio physical downlink control channel reliability enhancements for multiple transmission-reception-point communications," *IEEE Access*, vol. 10, pp. 97 394–97 407, Sep. 2022.
- [11] Y. Li, J. Pawlak, J. Price, K. Al Shamaileh, Q. Niyaz, S. Paheding, and V. Devabhaktuni, "Jamming detection and classification in OFDM-based UAVs via feature- and spectrogram-tailored machine learning," *IEEE Access*, vol. 10, pp. 16 859–16 870, Feb. 2022.
- [12] F. T. Zahra, Y. S. Bostanci, and M. Soyurk, "LSTM-based jamming detection and forecasting model using transport and application layer parameters in Wi-Fi based IoT systems," *IEEE Access*, vol. 12, pp. 32 944–32 958, Feb. 2024.
- [13] S. Sciancalepore, F. Kusters, N. K. Abdelhadi, and G. Oliveri, "Jamming detection in low-BER mobile indoor scenarios via deep learning," *IEEE Internet of Things Journal*, vol. 11, no. 8, pp. 14 682–14 697, Dec. 2024.
- [14] D. A. Tubail, M. Alsmadi, and S. Ikki, "Physical layer security in downlink of cell-free massive MIMO with imperfect CSI," *IEEE Transactions on Information Forensics and Security*, vol. 18, pp. 2945–2960, May 2023.
- [15] K. Zheng and X. Ma, "Designing learning-based adversarial attacks to (MIMO-)OFDM systems with adaptive modulation," *IEEE Transactions on Wireless Communications*, vol. 22, no. 9, pp. 6241–6251, Feb. 2023.
- [16] B. Tang and P. Stoica, "MIMO multifunction RF systems: Detection performance and waveform design," *IEEE Transactions on Signal Processing*, vol. 70, pp. 4381–4394, Aug. 2022.
- [17] "Study on channel model for frequencies from 0.5 to 100 GHz, document 3GPP TR 38.901, release 17," Mar. 2022.